Jurnal Teknik Sipil & Perencanaan 25 (2) (2023) p 190 – 198

JURNAL TEKNIK SIPIL & PERENCANAAN

10.15294/jtsp.v25i2.46357

# Experimental Study on The Capacity Of Z-Brace and X-Brace Cold-Formed Steel Wall Panel

Khristia Ningsih Cantikawati[1,] Nindyawati[2, a),] Roro Sulaksitaningrum[3]

[1,2.3]*Department of Civil Engineering and Planning Laboratory, Faculty of Engineering, Universitas Negeri Malang, Malang, Indonesia*

[a)]Corresponding author: nindyawati.ft@um.ac.id

**Abstract.** Awaludin et al. created an anti-earthquake temporary shelter called RISBARI (*Rumah Instan Baja Ringan*/Light Steel Instant House), featuring an X-shaped strap-braced wall system using cold-formed steel as its primary structure. A similar temporary shelter (*hunian sementara*/huntara) was developed by Biru Bumi Hijau using Z-shaped wall bracing. While experimental research on the lateral strength of cold-formed steel wall panels with X-brace bracing, such as in RISBARI, has been conducted extensively, there has been limited in-depth study on Biru Bumi Hijau's huntara. Hence, this research aimed to identify the load capacity, stiffness, and ductility of both bracing configurations on lateral strength using cold-formed steel wall panels. This study used an experimental method through the monotonic static load in the laboratory. The test results were analyzed with One-way ANOVA. The load capacity, stiffness, and ductility of the X-brace panel increased by 201%, 4452%, and 105%, respectively. In contrast, the load capacity, stiffness, and ductility of the Z-brace panel increased by 201%, 4253%, and 156%. The bracing capacity on both was not directly proportional since both test objects had different configuration structures, although they had equalized length and width.

**Keywords:** Lateral Strength, Cold-Formed Steel Panel, X-brace, Z-brace, *X-Brace*, *Z-Brace*, Static Monotonic

## INTRODUCTION

Indonesia is prone to geological disasters, with earthquakes being a major concern. Geological Agency inspections conducted from 2000 to 2021 show that destructive earthquakes had occurred 5 to 26 times in Indonesia. Providing earthquake-resistant temporary housing for disaster victims is a crucial solution to offer survivors a sense of security while safeguarding them against potential future disasters [1].

The structure follows the Capacity Design concept, determining specific structural elements that will yield under seismic stress, while other elements remain elastic to prevent structural collapse, even when damaged by an earthquake[2]. One implementation of this concept is the Concentric Bracing Frame System (Sistem Rangka Bresing Konsentris/SRBK), often used with cold-formed steel profiles, as evidenced in [3] and [4]. RISBARI (*Rumah Instan Baja Ringan*/Light Steel Instant House) is an earthquake-resistant temporary shelter created by [4]. It features an X-shaped strap-braced wall system using cold-formed steel as the main structural component. Many experimental studies have been conducted on the lateral strength of RISBARI's strap-braced cold-formed steel walls, as evidenced in [5] and [6]. However, similar Z-shaped wall stiffeners in temporary shelters developed by [7] did not have an in-depth experimental study.

Differences in bracing configurations that affect the stiffness of cold-formed steel wall require more specific study to assess their effectiveness. [8] obtained a result that stated that the steel X-brace type was the most optimal; however, it remains unclear whether these results hold true when examining various cold-formed steel bracing configurations. Diagonal bracing testing was also conducted by [9] with a test procedure based on [10].

This study aimed to identify the most optimal bracing to receive lateral loads when modeled as cold-formed steel wall panels. It builds upon prior research, addressing the gaps in previous discussions. The study was reviewed through capacity parameters, including peak load, stiffness, and structural ductility, compared through several models X-braced, Z-braced, and blank panel as a comparison. Here, the specimen capacity test was carried out by physical testing in the laboratory using the monotonic static loading method.

# RESEARCH METHODOLOGY

## Specimen Planning

Specimen were prepared using cold-formed steel material of the hollow box type measuring 40 mm x 40 mm with 0.3 mm thick**,** with a quality grade of G550. The profiles were arranged to form wall panels with concentric bracing connected at each gusset point. There were three specimen variations: wall panels with Z-brace, X-brace, and blank wall panels or without bracing (non-bracing). The wall panels were designed in 100 cm height and 50 cm width.

The Z-brace was configured, as seen in FIGURE 1, to have a total length and weight approximately equivalent to the X-brace. The measurements and weights for the Z-bracing were 448.6 cm and 1,583.5 gr, while the X-bracing was slightly shorter, measuring 433.6 cm in length and weighing 1530.6 gr. Code notations were given for each variation with 4 test objects each: S-X-1, S-X-2, S-X-3, S-X-4 for X-braced wall panels, S-Z-1, S-Z-2, S-Z-3, S-Z -4 for Z-braced wall panels, and S-0-1, S-0-2, S-0-3, S-0-4 for non-braced wall panels.

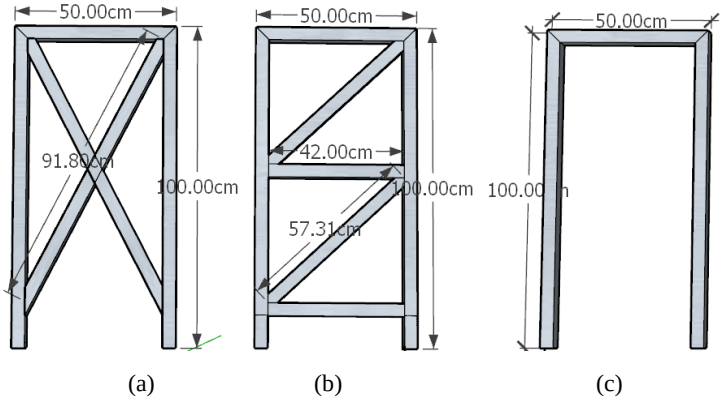


**FIGURE 1.** Test Object Design: (a) *X-Brace*, (b) *Z-Brace*, (c) *Non-brace*

## Instrumentation and Test Setup

Monotonic static testing in this study required mounting plate clamping to support accessories for the test object to avoid shifting. The clamping plate was designed following the length and width of the hollow box profile. A dial gauge was used to measure the pedestal displacement to ensure that the test went according to plan and that the clamp plate could clamp the test object properly. Millimeter block boards and pencils were also used to control test objects that would still experience displacement when given a load.

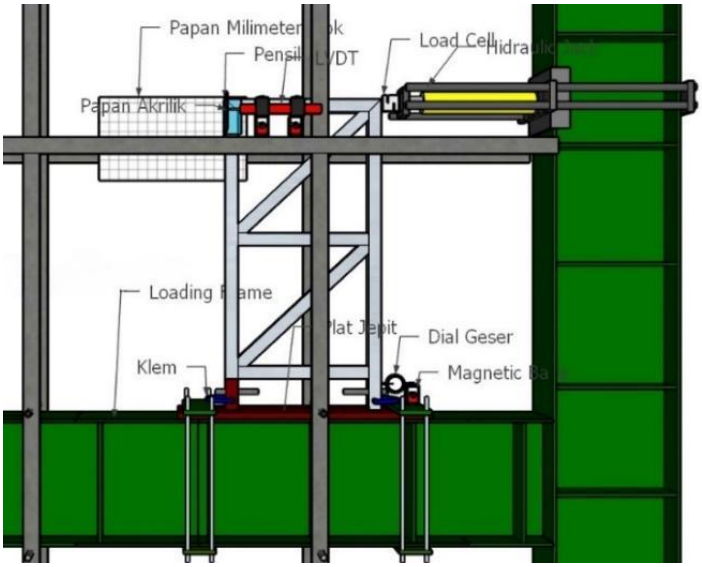


**FIGURE 2.** Monotonic Static Testing Setup

The test setup is illustrated in FIGURE 2. The hydraulic jack was positioned on the right side of the test object, moving from right to left to provide load, while the LVDT was placed parallel to the test object to measure its displacement. During the test, a manual form was used to record the results on the dial gauge at the lower end of the pedestal of each specimen. Meanwhile, digital LVDT did not require a form because the Displacement results would be recorded directly into Excel data via a data logger.

## Theoretical Basis

The monotonic static loading procedure was based on the rule [10]. Several capacity parameters were reviewed in this study, including Peak Load, Elastic Stiffness ($k_e$), and Ductility ($\mu$) values. FIGURE 3 shows the Equivalent Energy Elastic-Plastic (EEEP) curve, which is an approximation area of the relationship curve between the load-shear and the original envelope curve; its values can be affected by the axial Displacement and ultimate Displacement.

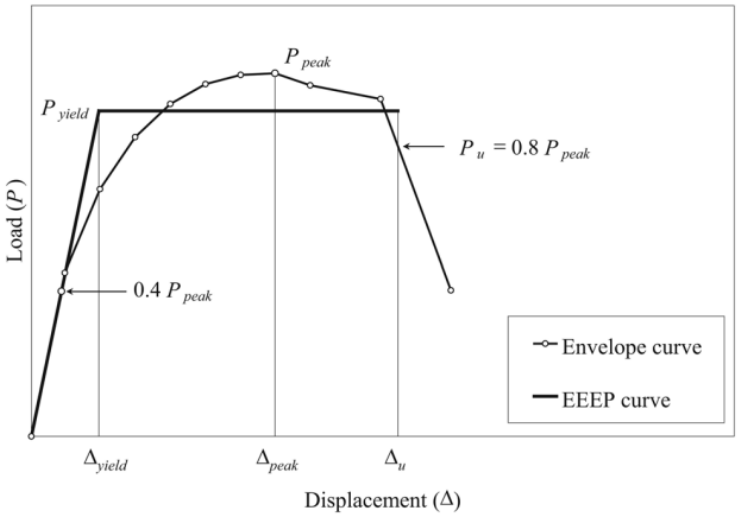


**FIGURE 3.** Envelope Curve and Equivalent Energy Elastic-Plastic Curve (EEEP)
Source*:* [10]

## Elastic Stiffness ($k_e$)

The elastic stiffness ($k_e$) can be known from the slope of the envelope curve when it reaches a load of 0.40 peak load ($P_{peak}$) and can also be used to calculate several parameters, namely yield load and yield Displacement. The formula to calculate the elastic stiffness according to [10] is as follows.

$$k_e = \frac{0{,}4\ P_{peak}}{\Delta\ 0{,}4\ P_{peak}} \quad \text{a)}$$

In which

$k_e$ = Elastic stiffness (kg/mm)
$0{,}40\ P_{peak}$ = Load during 0.40 $P_{peak}$ (kg)
$\Delta\ 0{,}40\ P_{peak}$ = Displacement at load 0.40 $P_{peak}$ (mm)

## Yield Displacement and Yield Load

The plastic part of the EEEP curve is the same horizontal line as the yield load ($P_{yield}$) and extends to the ultimate Displacement ($\Delta_u$), as illustrated in FIGURE 3. For the area of the load-displacement curve and the EEEP curve to be the same, look for the $P_{yield}$ value where the load curve-displacement area equals the EEEP curve area.

$$the\ P_{yield} = \left( \Delta_u - \sqrt{{\Delta_u}^2 - \frac{2A}{k_e}} \right) k_e \quad \text{b)}$$

In which:
$P_{yield}$ = Yield load (kg)
$\Delta_u$ = Ultimate Displacement (mm)
A = The area under the envelope curve (kg. mm)
$k_e$ = Elastic stiffness (kg/mm)
However, if ${\Delta_u}^2 < \frac{2A}{k_e}$, then allow to assume values with the following equation:

$$P_{yield} = 0{,}85\ P_{peak} \quad \text{c)}$$

After determining $P_{yield}$, yield Displacement can be measured using the:

$$\Delta_{yield} = \frac{P_{yield}}{k_e} \quad \text{d)}$$

In which:
$P_{yield}$ = yield load (kg)
$\Delta_u$ = ultimate Displacement (mm)

## Ductility

Finding ductility used the equation below, which is the ratio between the ultimate Displacement ($\Delta_u$) and the yield Displacement ($\Delta_{yield}$) based on the load (P)-Displacement ($\Delta$)relationship graph

$$\mu = \frac{\Delta_u}{\Delta_{yield}} \quad \text{e)}$$

In which:
$\mu$ = Ductility
$\Delta_u$ = Displacement during 0.80 $P_{peak}$ loads (mm)
$\Delta_{yield}$ = Displacement during first yield (mm)

## RESULT AND DISCUSSION

The monotonic static loading data on cold-formed steel wall panels consisted of three variations: blank or non-brace panels, X-brace, and Z-brace, with four specimens in each variation. Tests were carried out at intervals of every 2 kg until the specimen experienced a load reduction up to 40% of the obtained peak load. From the monotonic static

loading, some data were generated as loads and Displacements so that the envelope and EEEP curves were arranged as follows:

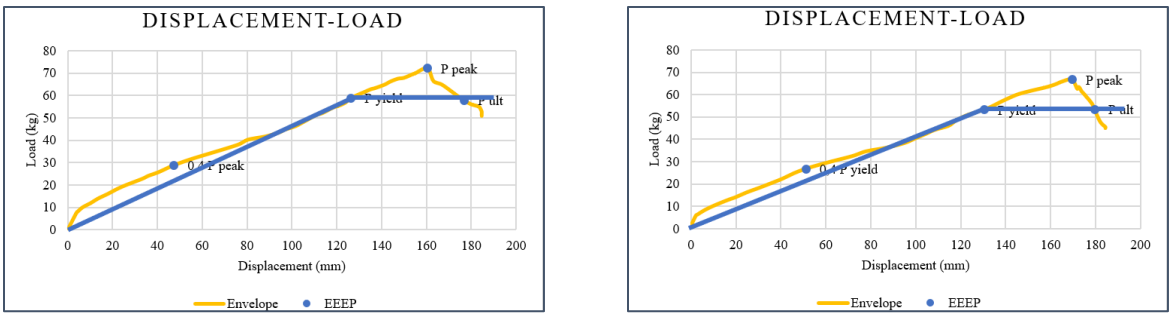


**FIGURE 4.** Non-brace Load-Displacement Curve and the EEEP Curve: a) S-0-1 and b) S-0-2

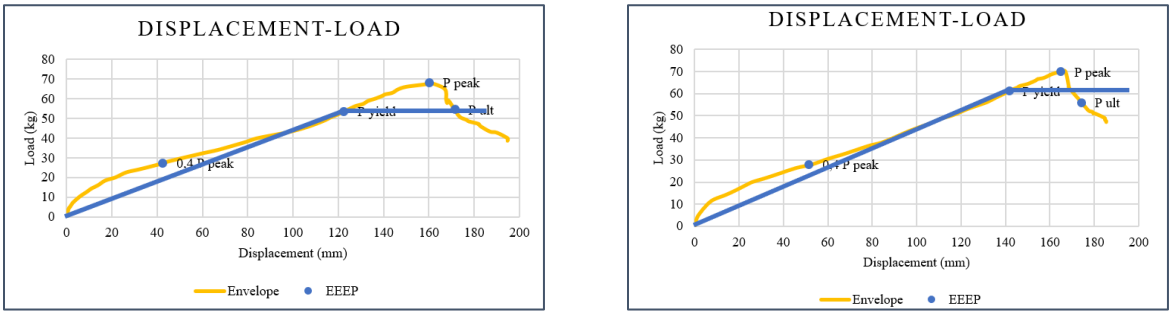


**FIGURE 5.** Non-brace Load-Displacement Curve and the EEEP Curve: a) S-0-3 and b) S-0-4

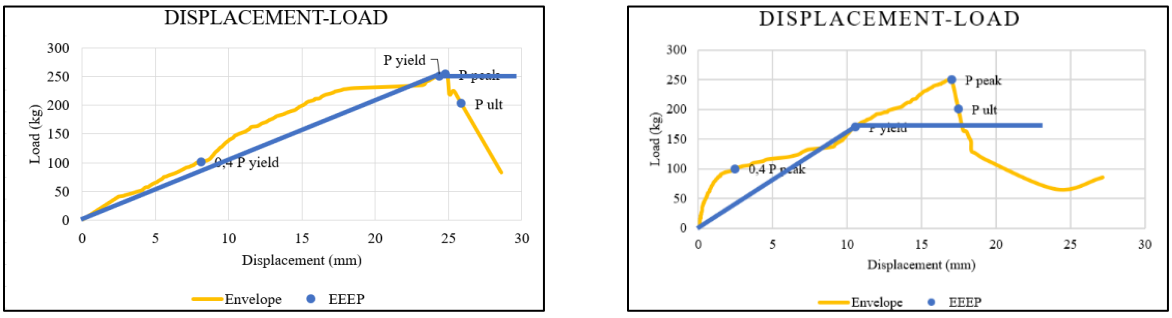


**FIGURE 6.** X-brace Load-Displacement Curve and the EEEP Curve: a) S-X-1 and b) S-X-2

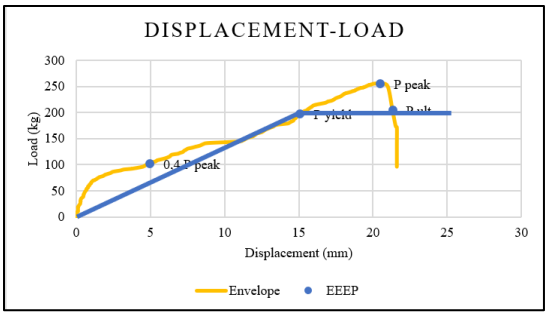


a)

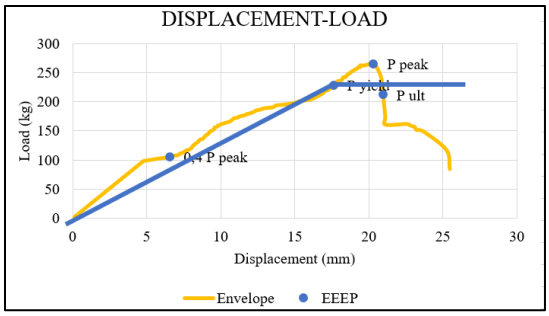


b)

**FIGURE 7.** X-brace Load-Displacement Curve and the EEEP Curve: a) S-X-3 and b) S-X-4

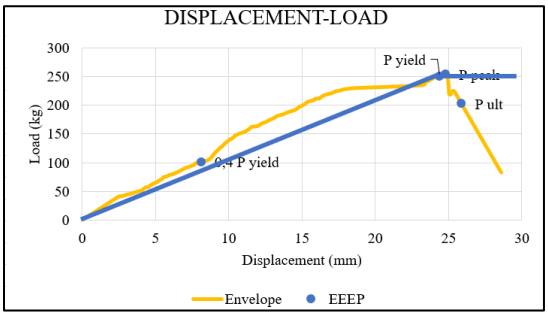


a)

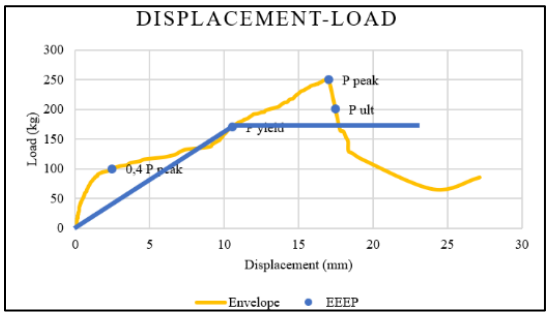


b)

**FIGURE 8.** Z-brace Load-Displacement Curve and the EEEP Curve: a) S-X-1 and b) S-X-2

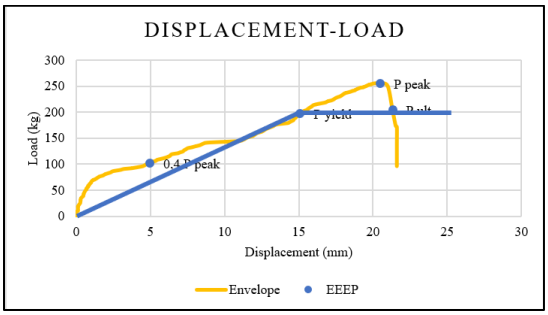


c)

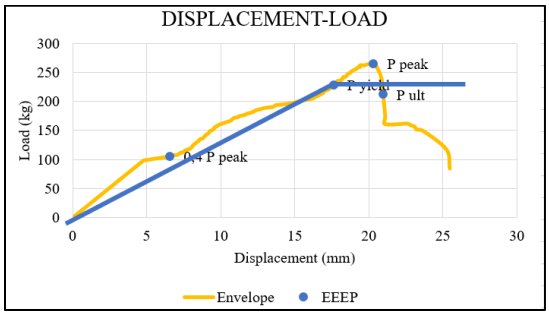


d)

**FIGURE 9.** Z-brace Load-Displacement Curve and the EEEP Curve: a) S-X-3 dan b) S-X-4

From the data analysis using One-Way ANOVA, the outlier data or data that deviated to the right or left it caused a more significant standard deviation between each variation. The following table presents test results and monotonic static test calculations after reducing the outlier data.

**TABLE 1.** Test Results and Monotonic Static Tests Calculations Recapitulation

| Test Object Code | 0.4 P peak (kg) | P yield (kg) | P peak (kg) | P ult (kg) | 0.4 Δ peak (mm) | Δ yield (mm) | Δ peak (mm) | Δ ult (mm) | A (kg. mm) | $K_e$ (kg/ $mm^2$) | μ |
|---|---|---|---|---|---|---|---|---|---|---|---|
| S-0-1 | 28.912 | 58.912 | 72.280 | 57.824 | 47.463 | 126.395 | 160.400 | 176.913 | 7573.554 | 0.609 | 1.400 |
| S-0-2 | 26.728 | 53.360 | 66.820 | 53.456 | 51.152 | 130.517 | 169.600 | 179.635 | 6860.741 | 0.523 | 1.376 |
| S-0-3 | 27.352 | 53.612 | 68.380 | 54.704 | 42.497 | 122.449 | 160.220 | 171.439 | 6958.328 | 0.644 | 1.400 |
| S-0-4 | 27.976 | 61.266 | 69.940 | 55.952 | 51.580 | 141.741 | 165.040 | 174.253 | 7215.569 | 0.542 | 1.229 |
| S-X-2 | 100.256 | 170.855 | 250.640 | 200.512 | 2.468 | 10.564 | 17.020 | 17.462 | 2624.119 | 40.622 | 1.653 |
| S-X-3 | 102.128 | 197.149 | 255.320 | 204.256 | 4.955 | 15.098 | 20.500 | 21.324 | 3261.152 | 20.612 | 1.412 |
| S-X-4 | 106.184 | 228.978 | 265.460 | 212.368 | 6.574 | 17.617 | 20.320 | 20.956 | 3175.440 | 16.153 | 1.189 |
| S-Z-1 | 84.240 | 201.684 | 210.600 | 168.480 | 2.714 | 9.576 | 28.540 | 29.297 | 5253.549 | 31.045 | 3.060 |
| S-Z-3 | 82.992 | 182.816 | 207.480 | 165.984 | 3.241 | 8.079 | 9.520 | 9.875 | 1152.846 | 25.609 | 1.222 |
| S-Z-4 | 82.888 | 189.410 | 207.220 | 165.776 | 4.800 | 13.346 | 25.520 | 27.030 | 4080.947 | 17.267 | 2.025 |

Based on TABLE 1, the capacity parameter values of each variation can be observed, including peak load ($P_{peak}$), stiffness ($k_e$) and ductility (μ). The mean and percentage of the three parameters for each variation of the test specimen are as follows.

**TABLE 2.** Increase of Bracing Configuration Variation Capacity Parameters to Control

| Test Object Code | Average $P_{peak}$ (kg) | Increase Percentage of $P_{peak}$ (%) | Average $k_e$ ($kg/mm^2$) | Increase the Percentage of $k_e$ (%) | Average μ | Increase Percentage of μ (%) |
|---|---|---|---|---|---|---|
| *Non-brace* (0) | 69.355 | 100% | 0.579 | 100% | 1.351 | 100% |
| *X-brace* | 257.140 | 371% | 25.796 | 4452% | 1.418 | 105% |
| *Z-brace* | 208.433 | 301% | 24.640 | 4253% | 2.102 | 156% |

Based on TABLE 2, the X-brace and Z-brace experienced increased capacity due to the additional bracing through the control test object or the non-brace panel. The peak load results above follow [11] and [12], in which the X-brace configuration could withstand tremendous lateral loads. This correlated to the diagonal stiffeners, which were in a crossed state; in the event of a lateral force such as wind or seismic activity, one of the members would be under tensile stress while the other is compressed according to the landing direction. In the Z-brace, when a lateral force occurred, the only thing that worked was the compression rod because it did not have a diagonal rod on the reverse side. Referring to research [13], horizontal bars such as the Z-brace configuration would only be more effective if used to withstand axial loads or function similarly to beams as Moment-Resisting Frame (MRF).

The stiffness value was also directly proportional to the peak load; in other words, the X-brace panel was still superior even though the stiffness magnitude was not too significant, only 1.156 kg/mm higher. This can be explained as the two test variations had similar diagonal bars even with different configurations; therefore, the stiffness was identical as long as the applied load direction was close to the anchor point of the diagonal bracing on the structure. This is supported by [14], which analyzed the performance of the V-brace structure. The V-brace had two diagonal rods in opposite directions, so the two rods carried horizontal compressive loads equally when seismic or alternating forces were applied from both directions.

While the third parameter, ductility, was not directly proportional to the two previous parameters. The X-brace ductility was less than the Z-brace. According to [15], the X-brace frame structure generally has large slenderness. It has tension-only property or more dominant tensile stress and causes the bracing to buckle even with a small load

easily. Therefore, the inelastic ability of the X-brace frame due to cyclic loads is considered to be poor, so modifications are needed that contribute to the axial compressive strength, including by requiring a rigid connection on each X-bracing element and paying attention to the uniform cross-sectional size by applying Strong Colum Weak Beam. This modification in overcoming the deficiencies of the X bracing design system is supported by [16], which studied the improvement of design requirements to have better seismic behavior.

## CONCLUSION

- This study found that additional bracing to cold formed steel wall panels against peak loads due to lateral loads had a significant difference. Compared to control panel specimens without bracing, the X-brace panel had a peak load value of 271%, while the Z-brace panel only experienced an increase of 201%.
- The difference in the stiffness values of the X-brace and Z-brace configurations of cold-formed steel wall panels was directly proportional to the peak load obtained; the X-brace remained superior with an increase in stiffness of 4452% and Z-brace 4253%.
- The addition of cold-formed steel wall panel X-brace and Z-brace configuration bracing on ductility due to lateral loads with no significant effect. It was not directly proportional to the peak load and stiffness obtained. According to [17], the X-brace was included in low ductility (<2), while the Z-brace was classified as medium ductility (2–5).

## REFERENCES


[1] N. I. R.A and G. P. Adhitama, "Tinjauan Karakter Shelter Sementara Sebagai Upaya Mitigasi Bencana Bagi Korban Bencana Alam," *Serat Rupa Journal of Design*, vol. 5, no. 2, pp. 270–287, doi: 10.28932/srjd.v5i2.3014, 2021.

[2] K. Sudarsana, M. Ery, and A. Yudha, "Pengaruh Rasio Kekakuan Lateral Struktur Terhadap Bertingkat Rendah," *Simposium Nasional RAPI XIII - 2014 FT UMS*, pp. 7–13, 2014.

[3] G. Di Lorenzo and A. De Martino, "Earthquake Response of Cold-Formed Steel-Based Building Systems : An Overview of the Current State of the Art," *Buildings*, vol. 9, no. 228, 2019.

[4] A. Awaludin, Y. Adiyuano, and F. A. Mursyid, "RISBARI: An alternative house model for the 2018 Lombok earthquake affected people," *IOP Conf Ser Mater Sci Eng*, vol. 849, no. 1, doi: 10.1088/1757-899X/849/1/012069, 2019.

[5] A. Kadir *et al.*, "Kekuatan Lateral Dinding Cold-Formed Steel Strap-braced Pada Rumah Instan Sehat Baja Ringan (RISBARI)," pp. 136–143, 2021.

[6] B. Hamdani, I. Satyarno, H. Priyosulistyo, J. Grafika, N. Kampus, and U. G. M. Yogyakarta, "Kapasitas Panel Rumah Instan Sehat Baja Ringan (RISBARI)," 2018.

[7] Biru Bumi Hijau, "Panduan Membangun Hunian Sementara (Rangka Galvalume, Dinding Kalsiboard, Atap Zincalume) uk 3,6M X 6M." Surabaya, 2019.

[8] I. M. S. W. Pangestu, A. Wibowo, and M. N. W, "Analisis Statik Non-Linier Pushover Pada Optimalisasi Desain Gedung Pendidikan Bersama FKUB Dengan Variasi Konfigurasi Bresing Baja," *Jurusan Teknik Sipil*, 2017.

[9] F. Monika and D. A. Awaludin, "Studi Kuat Geser Panel Kayu Vertikal Dengan Perkuatan Single Bracing Tulangan Baja Akibat Pembebanan Monotonik," *Rekayasa Sipil*, vol. 6, no. 2, pp. 60–67, 2017.

[10] ASTM E2126, "Standard Test Methods for Cyclic (Reversed) Load Test for Shear Resistance of Vertical Elements of the Lateral Force Resisting Systems for Buildings," no. C. pp. 1–14, doi: 10.1520/E2126-11.2, 2012.

[11] S. Haryono, D. Arumningsih, and D. Purnamawanti, "Penggunaan Struktur Bresing Konsentrik Tipe X Untuk Perbaikan Kinerja Struktur Gedung Bertingkat Terhadap Beban Lateral Akibat Gempa," *Jurnal Teknik Sipil Dan Arsitektur*, vol. 16, no. 2, 2015.

[12] I. Made Surya Wisnu Pangestu, A. Wibowo, and M. W. Narto, "Analisis Statik Non-Linier Pushover Pada Optimalisasi Desain Gedung Pendidikan Bersama Fkub Dengan Variasi Konfigurasi Bresing Baja," 2017.

[13] S. V. Tiffany, "Modifikasi Perencanaan Struktur Gedung Hotel Swiss-Bell Yogyakarta Menggunakan Struktur Baja Beton Komposit Dengan Sistem Rangka Bressing Konsentris Khusus," Institut Teknologi Sepuluh Nopember, 2018.

[14] J. A. Repadi, J. Sunaryati, and R. Thamrin, “Analisis Kinerja Struktur Beton Bertulang Dengan Variasi Penempatan Bracing Inverted V,” *Jurnal Rekayasa Sipil (JRS-Unand)*, vol. 12, no. 2, p. 103, 2016, doi: 10.25077/jrs.12.2.103-110.2016.
[15] M. Bruneau, C.-M. Uang, and R. Sabelli, *Ductile Design of Steel Structures*, Second., vol. 39, no. 5, doi: 10.1201/9780203970843.ch73, 1998.
[16] A. Campiche and S. Costanzo, “Evolution of ec8 seismic design rules for x concentric bracings,” *Symmetry (Basel)*, vol. 12, no. 11, pp. 1–16, doi: 10.3390/sym12111807, 2020.
[17] ATC, “FEMA 306: Evaluation of Earthquake-Damaged Concrete and Masonry Wall Buildings,” doi: 10.1193/1.1586111, 1998.